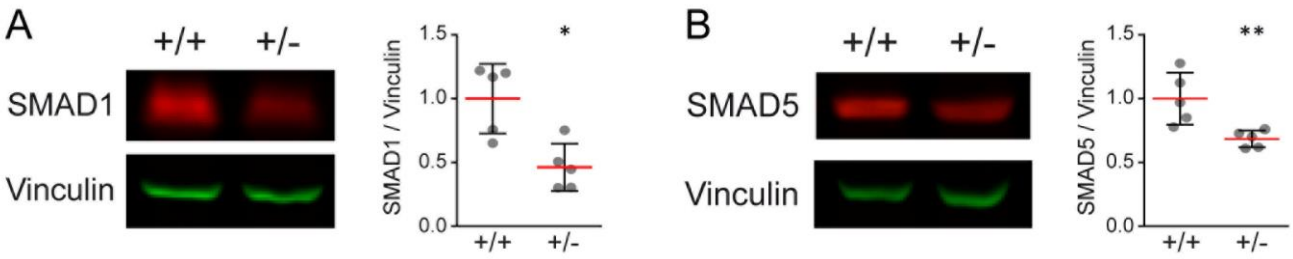

Figure S1: Reduction in SMAD1/5 protein levels in the SmadNes heterozygous mutant mouse.

(A-B) The levels of SMAD1 (A) and SMAD5 (B) proteins were assessed by Western blot in extracts obtained from telencephalons of E11.5 SmadNes heterozygous mutant embryos (*Smad1*$^{wt/fl}$;*Smad5*$^{wt/fl}$;*Nestin:Cre*$^{+/0}$, +/-) and their control littermates (*Smad1*$^{wt/fl}$;*Smad5*$^{wt/fl}$;*Nestin:Cre*$^{0/0}$, +/+), relative to the levels of Vinculin. The data represent the mean ratio ± s.d obtained from 5 mutant embryos and 5 control littermates. Significance was assessed with the non-parametric Mann–Whitney test (A, B). *P<0.05, **P<0.01.

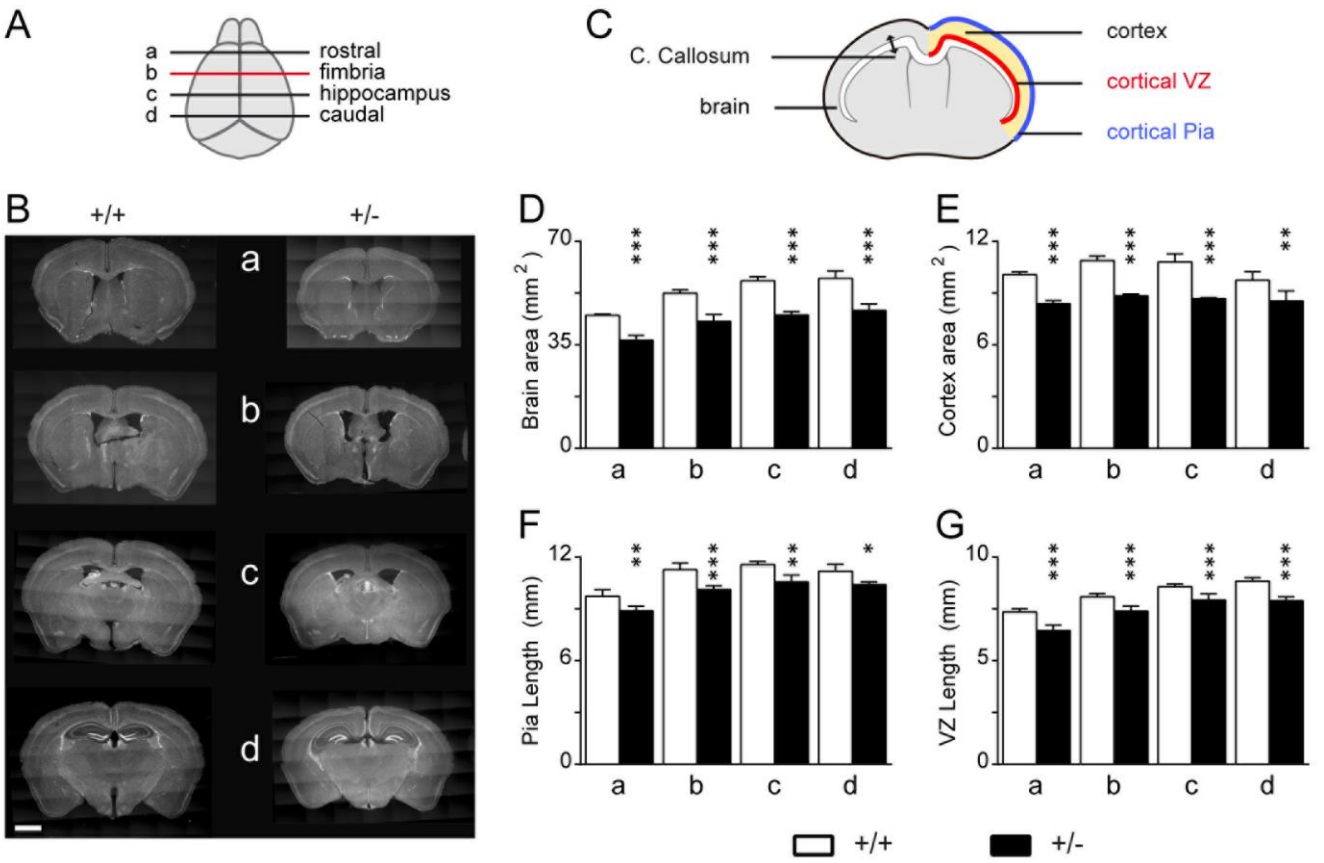

Figure S2: The size reduction of the adult SmadNes mutant brain is constant across the rostral-caudal axis.

(A) Representative rostral-caudal levels and (B) coronal sections of the adult brain (P60) of the SmadNes mutant mice (*Smad1*$^{wt/fl}$*;Smad5*$^{wt/fl}$*;Nestin:Cre*$^{+/0}$, +/-) and their control littermates (*Smad1*$^{wt/fl}$*;Smad5*$^{wt/fl}$*;Nestin:Cre*$^{0/0}$, +/+) in 4 different positions along the rostral-caudal axis (a to d, from rostral to caudal; b is also shown in Fig.1J), and (C) the distinct parameters analysed. (D,E) Mean area ± s.d of (D) the whole brain and of (E) the cerebral cortex. (F,G) Mean length ± s.d of (F) the cortical pia and of (G) the cortical VZ. n=5 embryos for +/+, n=3 for +/-. Significance was assessed with a two-way ANOVA + Sidak's test (D-G). *P<0.05, **P<0.01, ***P<0.001. Scale bar: 250 µm.

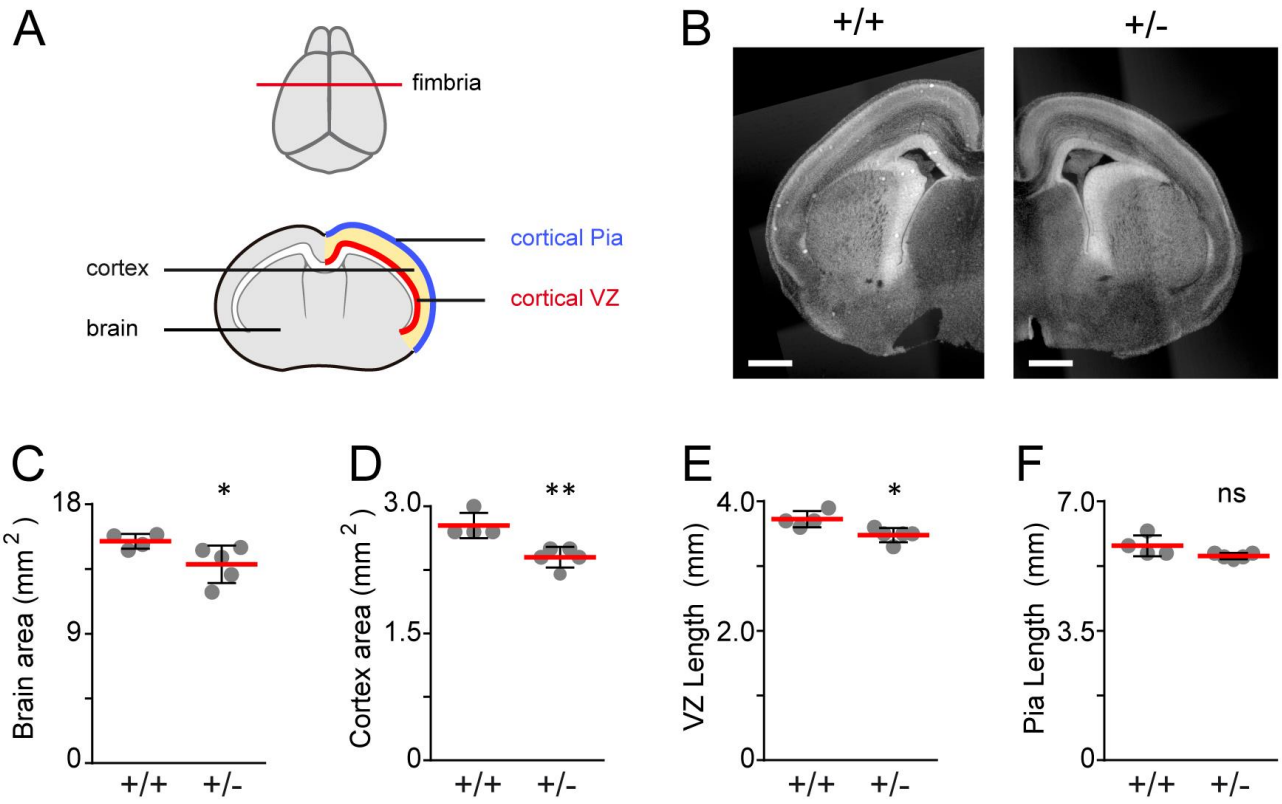

Figure S3: The size of the SmadNes mutant brain is reduced at the embryonic stage E17.5.

(A) Representative rostral-caudal level and the distinct parameters analysed on (B) coronal brain sections of E17.5 SmadNes mutant embryos (Smad1wt/fl;Smad5wt/fl;Nestin:Cre+/0, +/-) and control littermates (Smad1wt/fl;Smad5wt/fl;Nestin:Cre0/0, +/+). (C,D) Mean area ± s.d of (C) the whole brain and of (D) the cerebral cortex. (E,F) Mean length ± s.d of (E) the cortical VZ and of (F) the cortical pia, obtained from n=5 SmadNes mutant embryos (+/-) and 4 control littermates (+/+). Significance was assessed with the non-parametric Mann-Whitney test (C-F). *P<0.05, **P<0.01, ns:P>0.05. Scale bar: 500 µm.

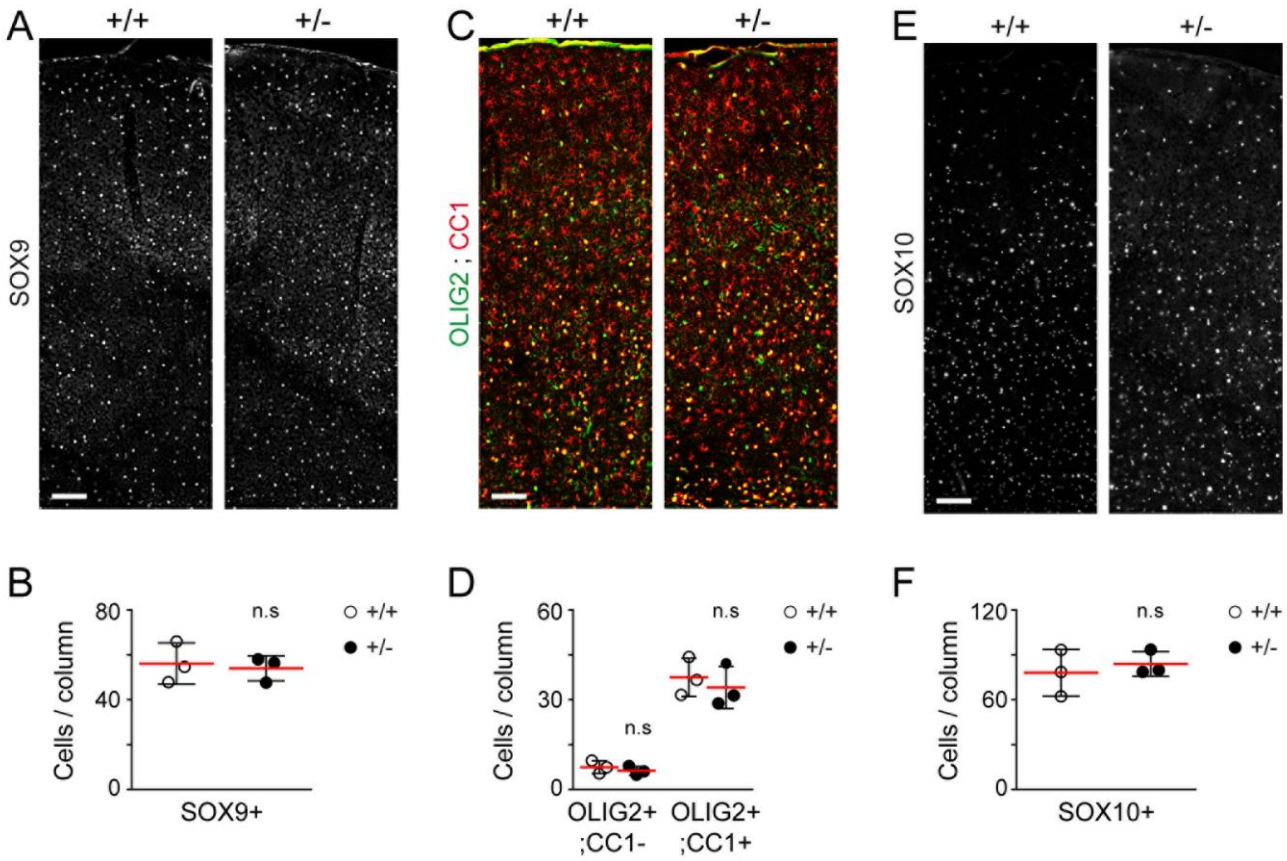

Figure S4: No alteration in the density of macroglial cells in the cerebral cortex of SmadNes mutant mice.

The density of macroglial cells present in the brains of SmadNes mutant mice (*Smad1*$^{wt/fl}$*;Smad5*$^{wt/fl}$*;Nestin:Cre*$^{+/0}$, +/-) and their control littermates (*Smad1*$^{wt/fl}$*;Smad5*$^{wt/fl}$*;Nestin:Cre*$^{0/0}$, +/+) was assessed in coronal sections at P60. (A, B) SOX9^{+} astrocytes and (C-F) oligodendroglial cells identified as (C, D) OLIG2^{+};CC1^{+} oligodendrocytes and their OLIG2^{+};CC1^{-} progenitors or as (E, F) SOX10^{+} oligodendroglial cells, and (B, D, F) their mean number ± s.d quantified in a 100 µm-wide radial column, obtained from 3 +/+ and 3 +/- animals. Significance was assessed with the non-parametric Mann–Whitney test. ns: P>0.05. Scale bars, 100 µm.

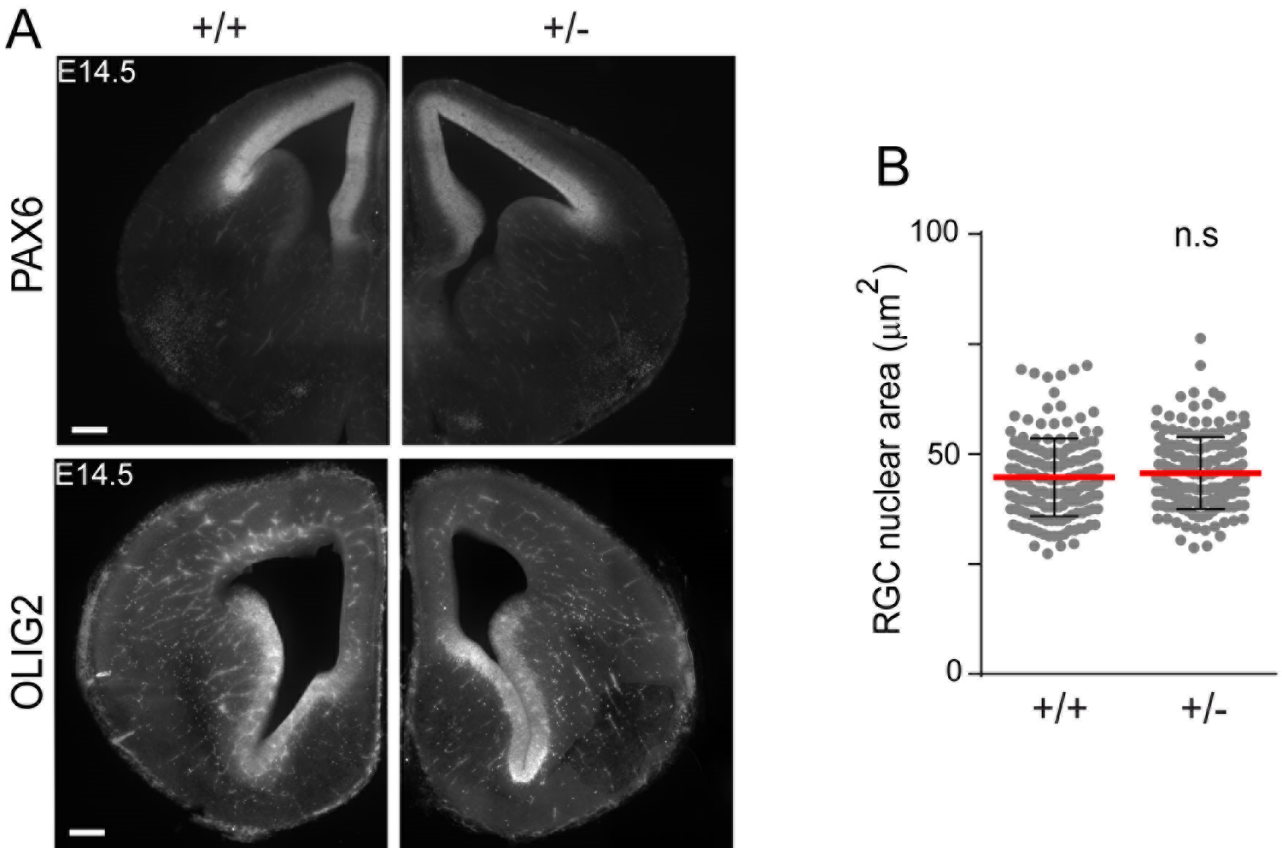

Figure S5: Absence of patterning and cell size defects in the cerebral cortex of SmadNes mutant embryos.

(A) Coronal sections immunostained for the pallial and sub-pallial patterning markers PAX6 and OLIG2 in the telencephalon of E14.5 SmadNes mutant embryos (*Smad1*$^{wt/fl}$*;Smad5*$^{wt/fl}$*;Nestin:Cre*$^{+/0}$, +/-) and their control littermates (*Smad1*$^{wt/fl}$*;Smad5*$^{wt/fl}$*;Nestin:Cre*$^{0/0}$, +/+). (B) Mean nuclear area ± s.d of the PAX6+;TBR2- RGCs in the ventricular zone of E11.5 SmadNes mutant embryos and control littermates, quantified in 170 cells derived from 5 embryos for each genotype. Each dot represents the value of 1 cell. Significance was assessed with the non-parametric Mann–Whitney test (B). ns: P>0.05. Scale bars, 100 µm.

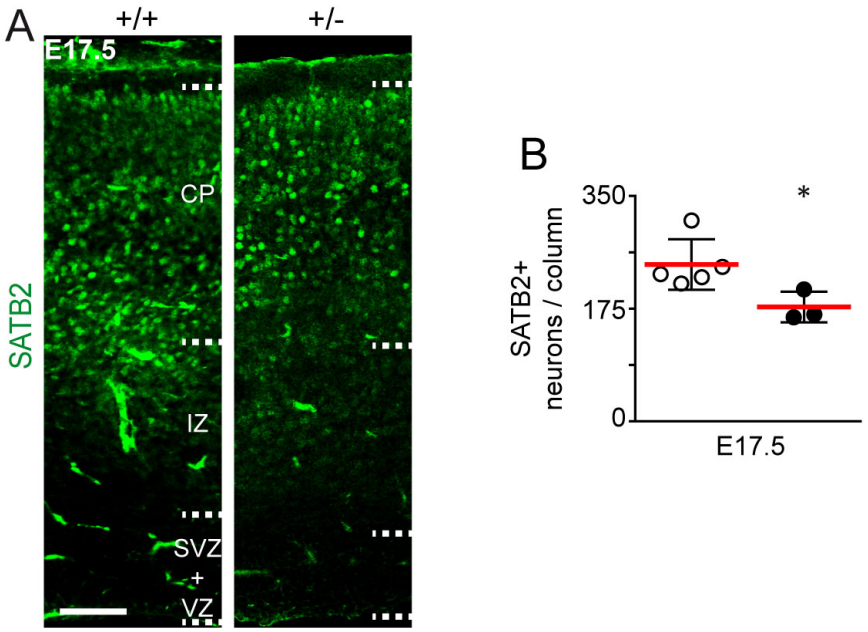

Figure S6: The number of SATB2+ neurons is decreased in the cerebral cortex of SmadNes mutant embryos.

(A) Immunostaining for SATB2, which reveals mid- and late-born projections neurons, in the developing cerebral cortex of E17.5 SmadNes mutant embryos (*Smad1*$^{wt/fl}$*;Smad5*$^{wt/fl}$*;Nestin:Cre*$^{+/0}$, +/-) and control littermates (*Smad1*$^{wt/fl}$*;Smad5*$^{wt/fl}$*;Nestin:Cre*$^{0/0}$, +/+). (B) Mean number of SATB2+ neurons ± s.d quantified in a 100 µm-wide cortical area, obtained from 5 +/+ and 3+/- embryos. Significance was assessed with the non-parametric Mann–Whitney test. *P<0.05. Scale bar, 50 µm. CP: cortical plate, IZ: intermediate zone, SVZ: sub-ventricular zone, VZ: ventricular zone.

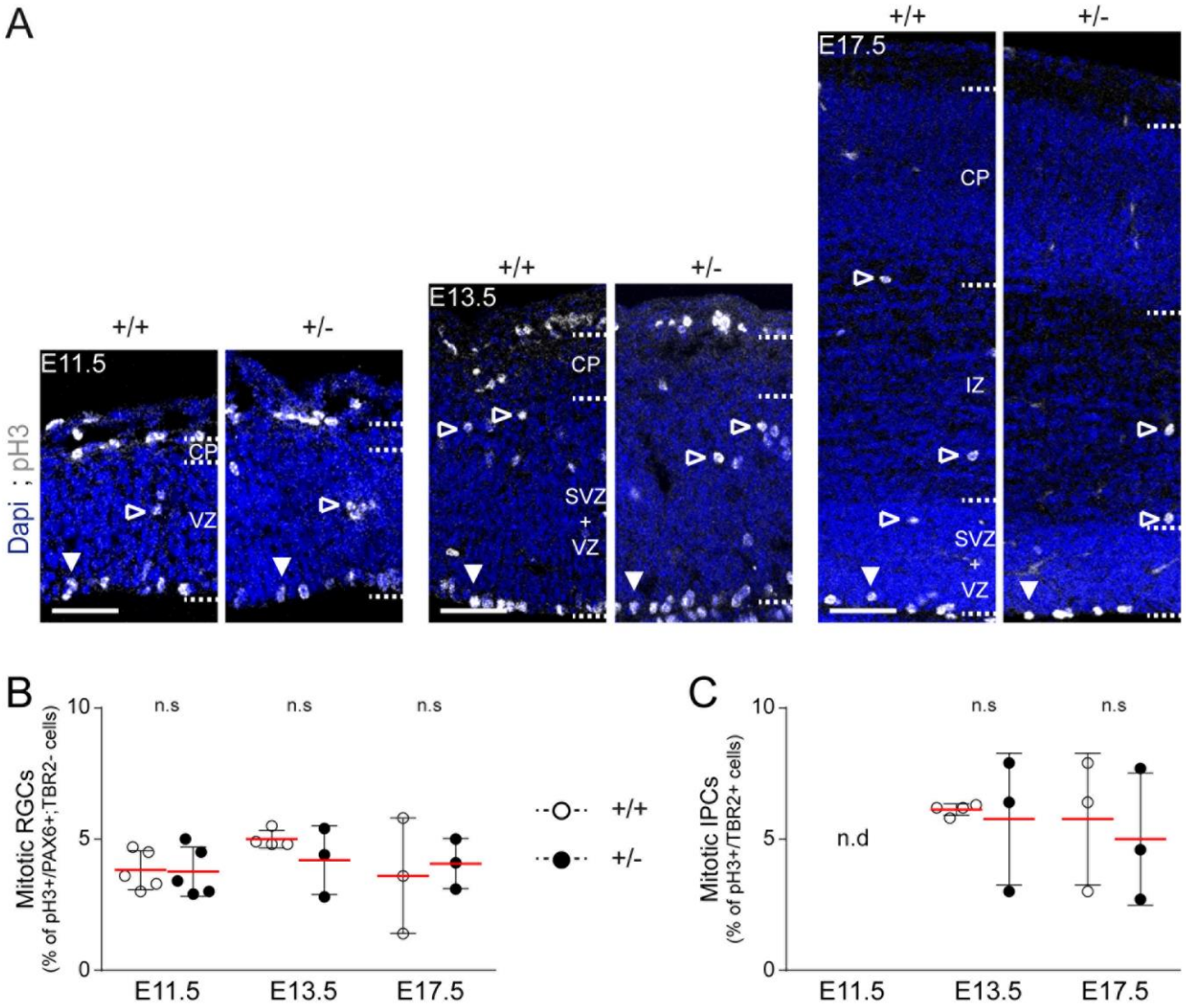

Figure S7: The mitotic index of RGCs and IPCs is not altered in the cerebral cortex of SmadNes mutant embryos.

(A) Coronal sections showing apical (white arrowheads) and basal (black arrowheads) pH3+ mitoses in the developing cerebral cortex of SmadNes mutant embryos (*Smad1*$^{wt/fl}$*;Smad5*$^{wt/fl}$*;Nestin:Cre*$^{+/0}$, +/-) and control littermates (*Smad1*$^{wt/fl}$*;Smad5*$^{wt/fl}$*;Nestin:Cre*$^{0/0}$, +/+) at E11.5, E13.5 and E17.5. (B, C) Mean proportion ± s.d of (B) pH3+/PAX6+;TBR2- cells (mitotic RGCs) and (C) pH3+/TBR2+ cells (mitotic IPCs) quantified in a 100 µm-wide cortical area, obtained from 5, 4, 3 +/+ and 5, 3, 3 +/- embryos at E11.5, E13.5 and E17.5, respectively. Significance was assessed at each developmental stage with the two-sided unpaired t-test. ns: P>0.05; nd: not determined. Scale bars, 50 µm. CP: cortical plate, IZ: intermediate zone, SVZ: sub-ventricular zone, VZ: ventricular zone.

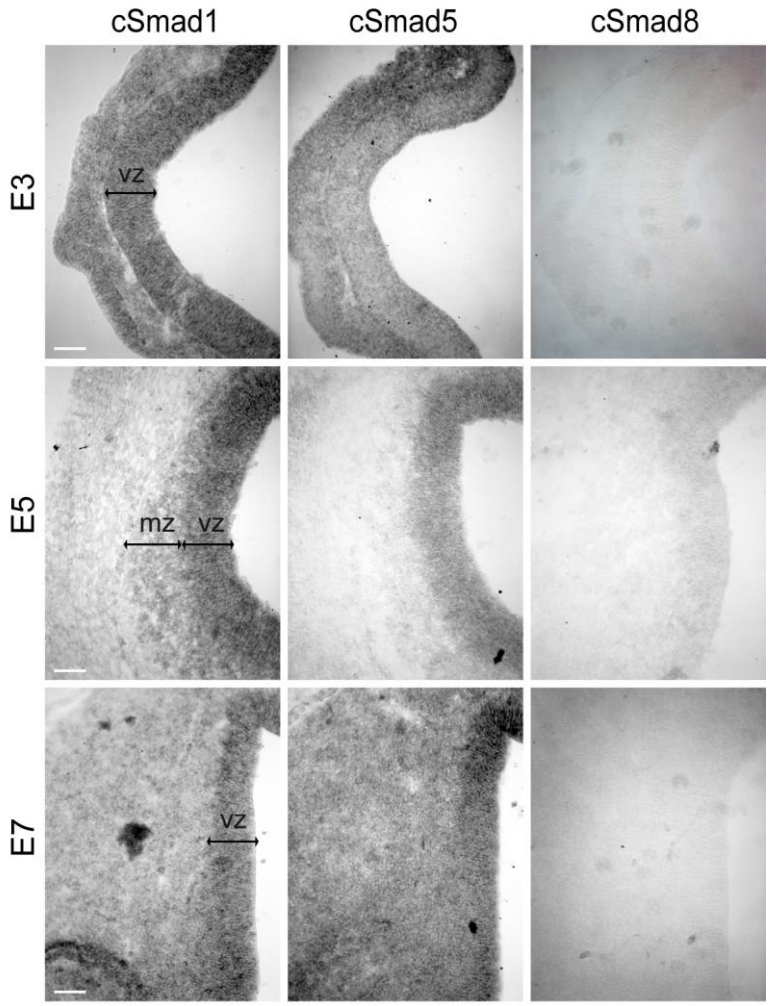

Figure S8: Expression of cSmad1/5/8 during chick cortical neurogenesis.

Coronal sections showing *cSmad1, cSmad5 and cSmad8* transcripts detected by in situ hybridization in the developing cerebral cortex of E3, E5 and E7 chick embryos. Scale bars: 50 µm. VZ: ventricular zone, MZ: mantle zone.

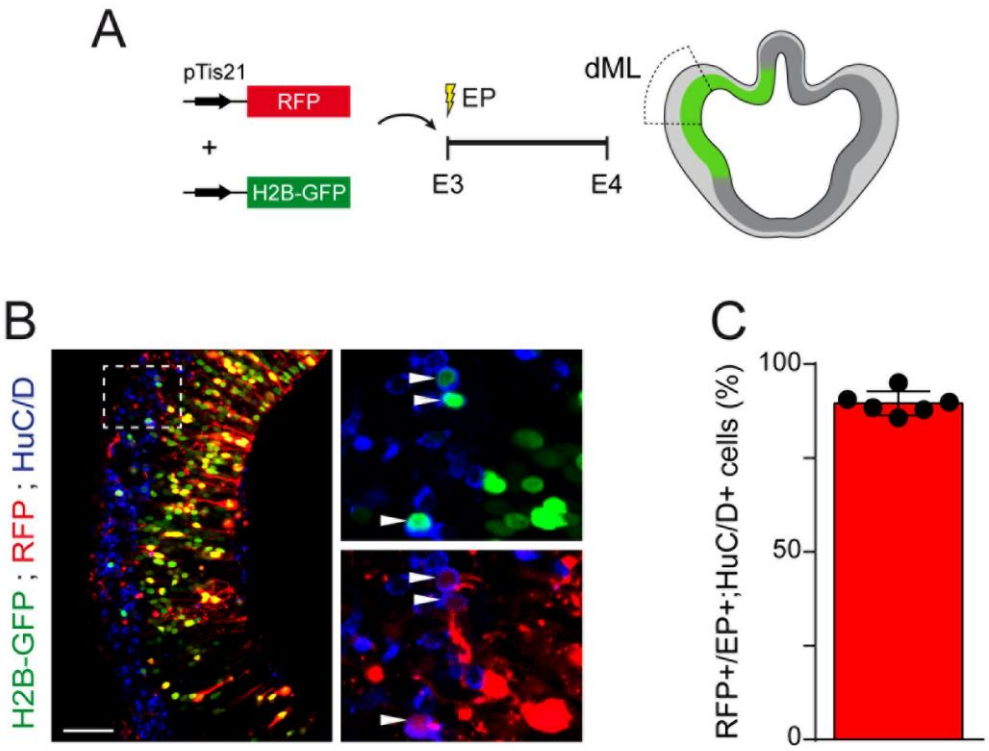

Figure S9: The activity of the pTis21:RFP reporter identifies neurogenic divisions during early chick cortical neurogenesis.

(A) Representation of the methodology used to identify neurogenic divisions during early chick cortical neurogenesis. The pTis21:RFP reporter was co-electroporated together with a constitutively active H2B-GFP-producing plasmid, and its activity assessed in the dorsal medial-lateral (dML) cortical region 24 hours after in ovo electroporation (IOE) of the dorsal telencephalon of E3 chick embryos. (B) Representative image of pTis21:RFP+ cells among the electroporated (H2B-GFP+) cells that differentiated into HuC/D+ neurons 24 hours later and (C) its quantification, presenting the mean proportion of RFP+ cells among H2B-GFP+;HuC/D+ cells ± s.d, obtained from 6 electroporated embryos. Scale bars: 50 µm.

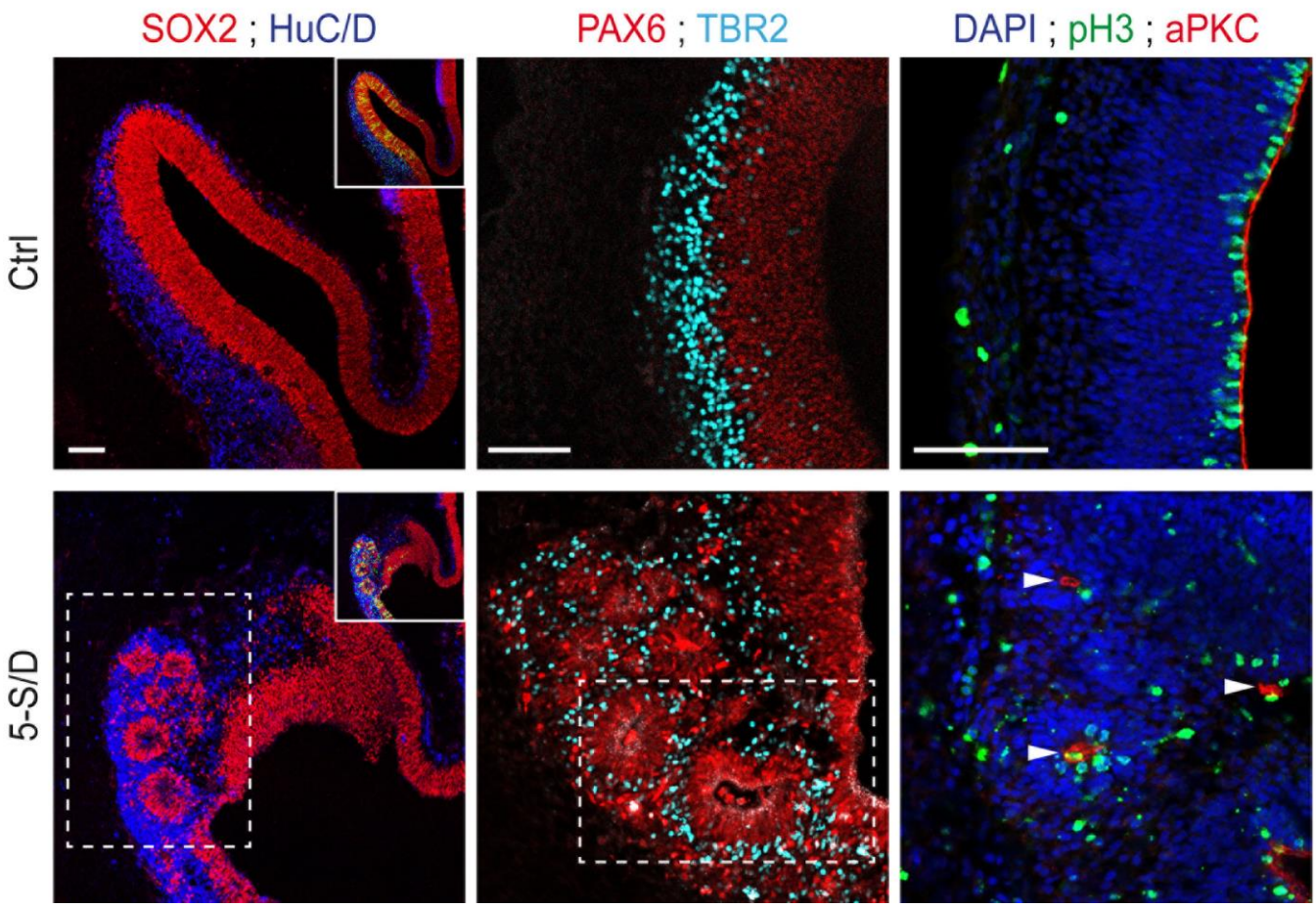

Figure S10: Increasing SMAD5 activity causes the abnormal generation of ectopic rosettes of cortical progenitors.

Representative images showing that IOE of SMAD5-S/D can cause the abnormal generation of ectopic rosettes of SOX2+ cortical progenitors. The PAX6+ and TBR2+ cells forming these rosettes developed an ectopic apical-basal polarity, as revealed by immunostaining for the apical marker atypical PKC (aPKC, arrowheads), and divide mostly at the center of the rosettes (pH3+). This phenotype has been observed in the cerebral cortex of 25% (5 out of 20) of the embryos electroporated with SMAD5-SD. Scale bars: 50 µm.

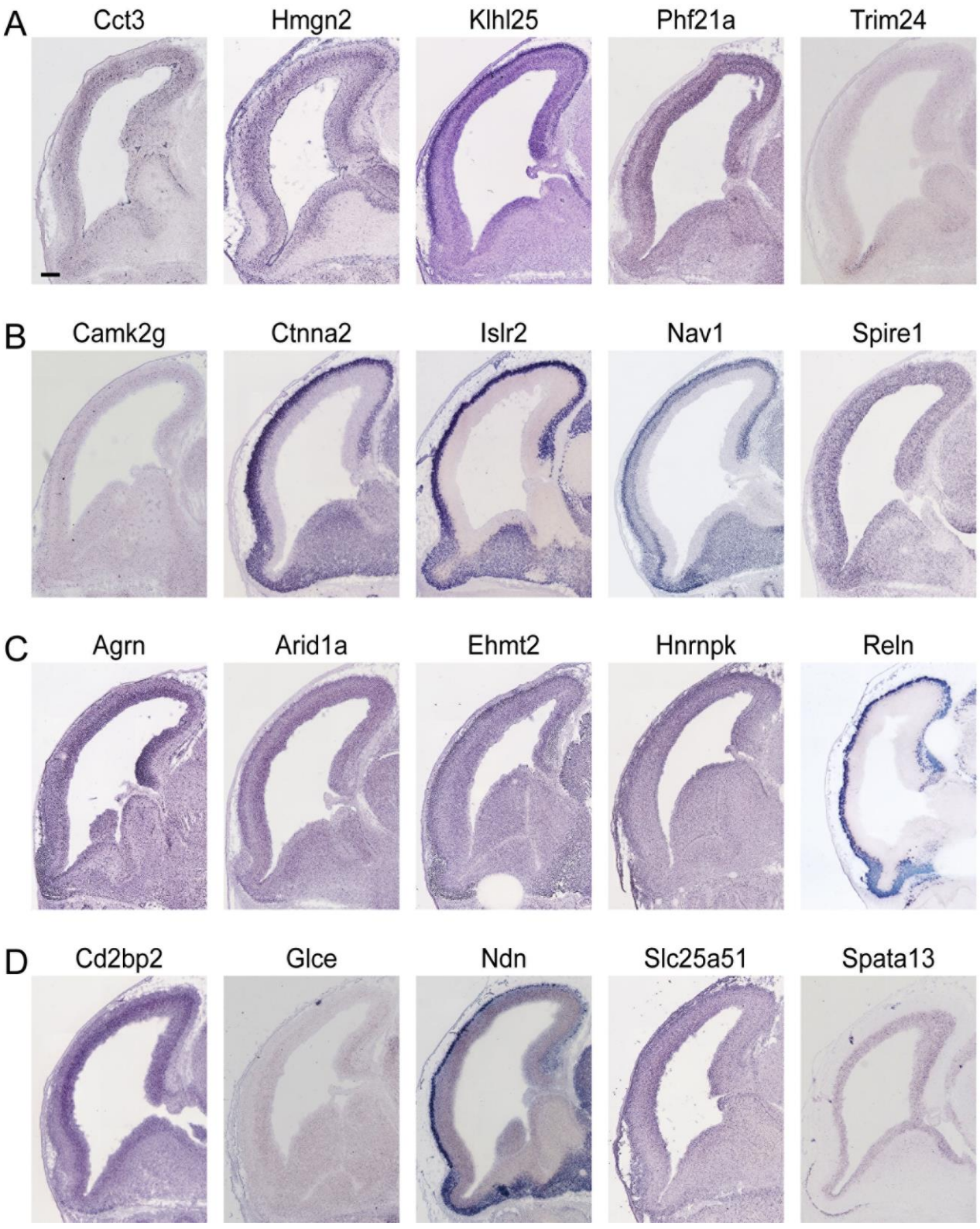

Figure S11: Gene expression pattern of RNAseq candidates in the mouse telencephalon.

Sagittal sections of the developing mouse dorsal telencephalon at E14.5 showing the gene expression pattern of candidates identified in the RNA-seq, including (A-C) genes whose promoters are enriched in binding motifs for TEADs and retrieved in the GO term related to (A) cellular biosynthesis such as *Cct3*,

Hmgn2, *Klhl25*, *Phf21a*, *Trim24*, (B) neurogenesis such as Camk2g, Ctnna2, Islr2, Nav1, Spire1, (C) both such as *Agrn*, *Arid1a*, *Ehmt2*, *Hnrnpk*, *Reln* and (D) genes not related to TEADs, such as *Cd2bp2*, *Glce*, *Ndn*, *Slc25a51*, *Spata13*. All the images were obtained from Genepaint (https://gp3.mpg.de). Scale bars: 50 µm.

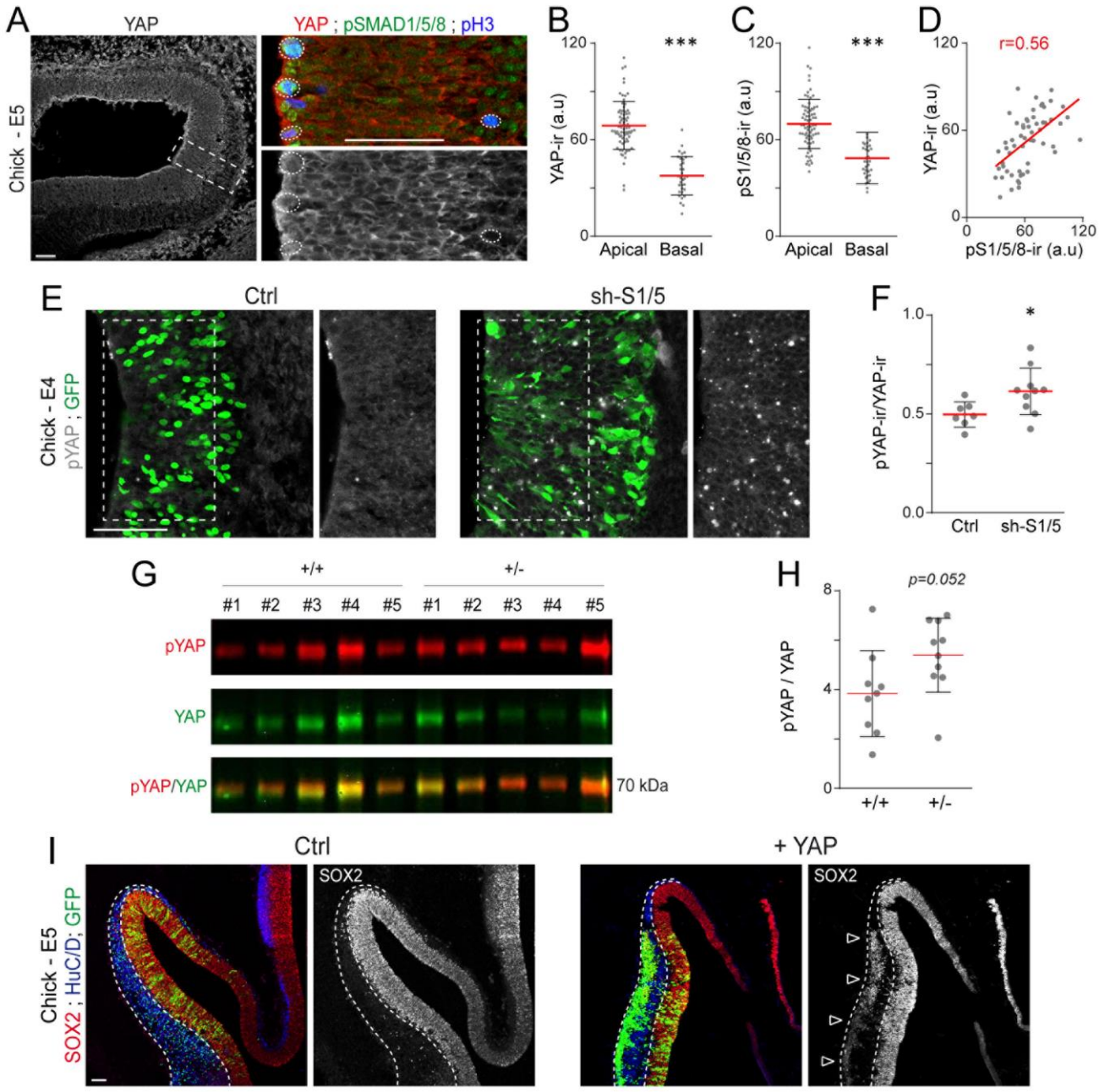

Figure S12: SMAD1/5 regulate early cortical neurogenesis through YAP.

(A) Expression of YAP during chick corticogenesis, relative to SMAD1/5 activity (pSMAD1/5/8). (B,C) The mean intensity ± s.d of endogenous YAP (B) and pSMAD1/5/8 (C) immunoreactivity was quantified in 74 apical and 33 basal mitotic (pH3+) nuclei obtained from 3 chick E5 embryos. (D) The correlation between the intensity of endogenous pSMAD1/5/8 and YAP immunoreactivities was assessed by calculating the Pearson's correlation coefficient r. (E) Immunostaining of the form of YAP phosphorylated at Serine 123 (pYAP) and (F) quantification of the mean ratio ± s.d of pYAP/YAP intensity obtained 24 hours after IOE with sh-S1/5 (10 sections from 3 embryos) or its control (7 sections from 3 embryos). (G) Western blot detection of the levels of pYAP and total YAP in extracts obtained from telencephalons of

E11.5 SmadNes mutant embryos (*Smad1*$^{wt/fl}$*;Smad5*$^{wt/fl}$*;Nestin:Cre*$^{+/0}$, +/-) and their control littermates (*Smad1*$^{wt/fl}$*;Smad5*$^{wt/fl}$*;Nestin:Cre*$^{0/0}$, +/+). (H) Quantification of the mean pYAP/YAP ratio ± s.d, obtained from 10 SmadNes mutant embryos (+/-) and 9 control littermates (+/+) derived from 2 different litters. (I) Immunostaining of the developing chick cerebral cortex for SOX2+ neural progenitors and HuC/D+ differentiating neurons 48 hours after IOE with a construct overexpressing the wild type form of YAP (YAP) or a control, showing that YAP overexpression can lead to a massive ectopic delamination of SOX2+ electroporated cells in the basal part of the mantle zone. Significance was assessed with the non-parametric Mann–Whitney test (B, C, F), the two-sided unpaired t-test (D, H).*P<0.05, ***P<0.001. Scale bars, 50 µm.

Table S1: List of differentially expressed transcripts between cortical RGCs from SmadNes mutant and control E12.5 embryos.

Click here to Download Table S1

Table S2: Gene ontology (GO) term enrichment analysis.

Click here to Download Table S2

Table S3: Transfac/Jaspar analysis and genes whose promoters are enriched in TEAD binding motifs.

Click here to Download Table S3

Table S4: Expression of the genes of the Hippo signalling pathway in cortical RGCs from SmadNes mutant and control E12.5 embryos.

Click here to Download Table S4

Antibody	Source	Dilution of use	Identifier
anti-aPKC (mouse)	Santa Cruz Biotechnologies	1:500	Cat #SC-17781 (H-1); RRID:AB_628148
anti-BrdU (rat)	AbD Serotec	1:100	Cat #MCA2060; RRID:AB_323427
anti-CC1/APC (mouse)	Millipore	1:200	Cat #OP80; RRID:AB_2057371
anti-CTIP2 (rat)	Abcam	1:500	Cat #ab18465; RRID:AB_2064130
anti-CUX1 (rabbit)	Proteintech	1:250	Cat #11733-1-AP; RRID:AB_2086995
anti-pHistone3 (rat)	Sigma Aldrich	1:1,000	Cat #H9908; RRID:AB_260096
anti-HuC/D (mouse)	Life Technologies	1:1,000	Cat #A-21271; RRID:AB_221448
anti-MEF2c (rabbit)	Abcam	1:500	Cat #ab64644; RRID:AB_2142861
anti-NeuN (mouse)	Millipore	1:500	Cat #MAB377; RRID: AB_2298772
anti-OLIG2 (rabbit)	Millipore	1:500	Cat #AB9610; RRID: AB_570666
anti-PAX6 (mouse)	DSHB	1:200	Cat #pax6; RRID:AB_528427
anti-PAX6 (rabbit)	Covance / Biolegend	1:100 (Ms) 1:250 (Chick)	Cat #901301; RRID:AB_2565003
anti-Prominin1 (rat) ; APC-conjugated	eBioscience	0.2 mg/ml	Cat #17-1331-81; RRID: AB_823120
anti-SATB2 (mouse)	Abcam	1:200	Cat #ab51502; RRID:AB_882455
anti-SMAD1 (rabbit)	Cell Signaling Technologies	1:1,000	Cat #6944S; RRID:AB_10858882
anti-SMAD5 (rabbit)	Cell Signaling Technologies	1:1,000	Cat #12534S; RRID: n.d
anti-pSMAD1/5/8 (rabbit)	Cell Signaling Technologies	1:250	Cat #9511; RRID:AB_331671
anti-SOX2 (rabbit)	Abcam	1:500	Cat #ab97959; RRID:AB_2341193
anti-SOX9 (rabbit)	Kindly provided by Dr. M. Wegner	1:500	RRID:AB_2315360
anti-SOX10 (goat)	R&D Systems	1:50	Cat #AF2864; RRID:AB_442208
anti-TBR1 (rabbit)	Abcam	1:250	Cat #ab31940; RRID:AB_2200219
anti-TBR2 (rabbit)	Abcam	1:200	Cat #ab23345; RRID:AB_778267
anti-TUBULIN-b3 (Tuj1) (mouse)	Covance	1:500	Cat #MMS-435P; RRID:AB_2313773
anti-Vinculin (mouse)	Sigma	1:20,000	Cat #V9131; RRID: AB_477629
anti-YAP (mouse)	Santa Cruz Biotechnologies	1:200	Cat #sc-101199; RRID:AB_1131430
anti-pYAP (rabbit)	Cell Signaling Technologies	1:1,000	Cat #4911; RRID:AB_2218913

Table S5: List of primary antibodies used in this study.